Zeolite HNU-87: synthesis, characterization and catalytic properties in the shape-selective conversion of methylnaphthalenes

Roger Gläser, Ruifeng Li, Michael Hunger, Stefan Ernst and Jens Weitkamp*

Institute of Chemical Technology I, University of Stuttgart, D-70550 Stuttgart, Germany

Received 26 August 1997; accepted 11 December 1997

The synthesis of the high-silica zeolite NU-87 and its physicochemical characterization are reported. The catalytic properties of zeolite HNU-87 were investigated in the conversion of 1- and 2-methylnaphthalene. Both isomerization to the corresponding methylnaphthalene and transalkylation to naphthalene and dimethylnaphthalenes are observed. The influence of reaction temperature and the modified residence time on the product distributions is reported and discussed in terms of shape selectivity effects in the peculiar pore system of NU-87. For comparison, typical results obained with zeolite HMCM-22, which possesses a similar pore architecture, are also included. The results of methylnaphthalene conversion over HNU-87 are compared to those obtained in the alkylation of naphthalene with methanol on the same zeolite catalyst.

Keywords: zeolite NU-87, synthesis, methylnaphthalene conversion, disproportionation, isomerization, shape selectivity

1. Introduction

Zeolite NU-87 is a high-silica zeolite which was first described by Casci and Stewart in 1990 [1]. Its pore system is built from parallel 10-membered-ring channels with a diameter of 0.47 nm×0.60 nm linked together by 12-membered-ring cavities which are accessible only via the 10-membered-ring windows of the channels [2,3]. This peculiar pore architecture renders zeolite NU-87 most attractive as a catalyst, especially for such conversions, in which the desired products are relatively slender (and can, hence, diffuse through the 10-membered-ring channels), but in which the transition states required for the formation of these desired products are relatively bulky, so that they can only be accommodated in larger void spaces, i.e., in the 12-membered-ring cavities or at channel intersections. One interesting example for such a type of reaction is the disproportionation of 2-methylnaphthalene (2-M-Np) to naphthalene and dimethylnaphthalenes. Among the dimethylnaphthalenes, the 2,6-isomer (2,6-DM-Np) is of special interest as a valuable intermediate in the production of high-temperature resistant polyesters and of liquid crystals.

While Fraenkel et al. [4,5] postulated that the shape-selective conversion of binuclear aromatics (e.g., the alkylation of 2-methylnaphthalene with methanol) on zeolite HZSM-5 occurs in so-called ''half cavities'' located at the external surface of the zeolite crystallites, it is now generally accepted that the shape-selective reactions of naphthalene derivatives at temperatures around 300°C occur *inside* the pore system of zeolite ZSM-5 as shown, e.g., by Weitkamp and Neuber [6]. The observed product distributions can be readily accounted for in terms of conventional shape selectivity effects, especially, if combined with a selectivation effect due to coke formation. Komatsu et al. [7] studied the effect of poisoning the acid sites located at the external surface of ZSM-5 crystallites by co-feeding 2,4-dimethylquinoline, as described earlier by Namba et al. [8]. Using this technique, Komatsu et al. were able to show that the isomerization of 2- to 1-methylnaphthalene and, likewise, the isomerization of 2,6- to 1,6-dimethylnaphthalene and of 2,7- to 1,7-dimethylnaphthalene occur at the external surface of the zeolite crystallites.

In the present study we report on the synthesis and physicochemical characterization of zeolite NU-87 and its catalytic properties in the Brønsted-acid catalyzed conversion of methylnaphthalenes. The results from the catalytic conversion of 2-methylnaphthalene are compared to those observed with zeolite MCM-22 which has a similar pore architecture (i.e., larger intracrystalline void spaces which are accessible by 10-membered-ring windows only) and to the behavior of zeolite HNU-87 in the alkylation of naphthalene with methanol.

2. Experimental

2.1. Synthesis of zeolite NU-87

Zeolite NU-87 was synthesized according to optimized procedures which were adapted from the literature [1,2]. In a typical synthesis, a solution of 0.38 g sodium aluminate (Riedel-de Haën, 54 wt% Al_2O_3, 41

* To whom correspondence should be addressed.

wt% Na_2O, rest: water) and 1.59 g sodium hydroxide (Merck) in 47 g water was combined with 22.2 g colloidal silica sol (Levasil, Bayer AG, 30 wt% SiO_2 in water) under stirring. A second solution containing 5.8 g decamethonium bromide ($DecBr_2$, decane-1,10-bis(trimethylammonium)dibromide, Fluka) in 37.5 g water was added under continuing stirring. The resulting gel had a molar composition of $55SiO_2 \cdot Al_2O_3 \cdot 11.5Na_2O \cdot 6.8DecBr_2 \cdot 2800H_2O \cdot 2.4NaBr$. For the crystallization of zeolite NU-87, the gel was transferred into a stainless steel autoclave with a volume of 300 cm^3 and rotated with a frequency of 30 min^{-1} at 180°C for 10 days. After rapid cooling the solid product was recovered by filtration, washed thoroughly with deionized water and dried at 120°C. To remove the organic template occluded during synthesis, the sample was calcined in air at 550°C (heating rate 2 K/min) for 2 days. The calcined material was ion-exchanged in a 1 n aqueous solution of NH_4NO_3 and dried at 120°C to obtain the ammonium form.

Zeolite MCM-22 was synthesized according to a procedure described previously [9]. The ammonium form was obtained from the calcined material in the same way as for zeolite NU-87.

2.2. Physicochemical characterization

X-ray powder diffraction patterns were collected on a Siemens D5000 instrument using Cu Kα radiation. The chemical composition of the samples was analyzed by atomic emission spectrometry with inductively coupled plasma (ICP-AES, Perkin-Elmer, Plasma 400). Thermal analysis (TGA/DTA) was conducted on a Setaram TG-DTA 92 instrument. A Bruker MSL 400 spectrometer was used for ^{13}C cross polarization (CP), ^{27}Al and ^{29}Si MAS NMR measurements. For the ^{27}Al measurements a 0.1 molar aqueous solution of aluminum nitrate and for the ^{13}C and ^{29}Si measurements tetramethylsilane (TMS) were used as external references, respectively. The resonance and MAS frequencies were 100.6 MHz and 4 kHz for ^{13}C, 104.3 MHz and 10 kHz for ^{27}Al and 79.5 MHz and 10 kHz for ^{29}Si experiments, respectively. For ^{13}C cross polarization, a contact time of 5 ms and a repetition time of 4 s were applied.

2.3. Catalytic experiments and temperature-programmed desorption of pyridine (TPDP)

The catalytic experiments were conducted under atmospheric pressure in a flow-type apparatus with a fixed-bed reactor. Nitrogen was used as the carrier gas. The calcined and ion-exchanged materials were pressed without binder, crushed and sieved to a particle size fraction of $d = 0.2$–0.3 mm. Prior to the experiments, the ammonium form of the zeolite was converted into the H^+-form in a purge of nitrogen ($\dot{V}_{N_2} = 30$ cm^3/min) at 400°C (or at the reaction temperature, whenever this was above 400°C) for 6 h. In a typical experiment, 2-methylnaphthalene ($p_{2\text{-M-Np}} = 0.2$ kPa) was passed over 0.2 g of catalyst at 300°C with a modified residence time of $W/F_{2\text{-M-Np}} \approx 2000$ g h/mol (WHSV = 0.07 h^{-1}). In the alkylation of naphthalene with methanol, two streams of carrier gas were loaded separately with vapors of naphthalene ($p_{Np} = 0.6$ kPa) and methanol ($p_{MeOH} = 0.4$ kPa), respectively, before being mixed and fed to the reactor. In both cases, the reaction products were analyzed by on-line sampling and temperature-programmed capillary gas chromatography (HP 5890, equipped with a 50 m capillary column coated with methyl silicone fluid and a flame ionization detector).

Temperature-programmed desorption of pyridine (TPDP) was performed using the same experimental setup. The samples (same particle size fraction and activation procedure as for the catalytic experiments) were loaded with pyridine ($p_{pyridine} = 1.3$ kPa) at 180°C in flowing nitrogen ($\dot{V}_{N_2} = 40$ cm^3/min) and were subsequently purged with pure nitrogen at the same temperature and flow rate to desorb physically bound pyridine. For the TPDP experiments, the loaded sample was heated with a rate of 5 K/min ($\dot{V}_{N_2} = 30$ cm^3/min) to 800°C, and the concentration of pyridine in the adsorber effluent was measured by on-line sampling and capillary GLC.

3. Results and discussion

3.1. Physicochemical properties of zeolite NU-87

The X-ray powder patterns of the as-synthesized and the calcined samples of zeolite NU-87 prepared in the present study are shown in figure 1. The peak positions and the relative intensities agree reasonably well with published data [1–3]. From a comparison with the recently reported powder pattern of zeolite SSZ-37 [10]

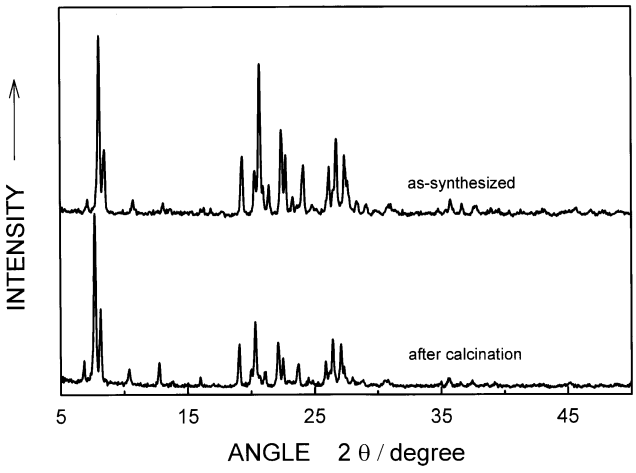

Figure 1. X-ray powder diffraction patterns of zeolite NU-87 in the as-synthesized form and after calcination at 550°C in air.

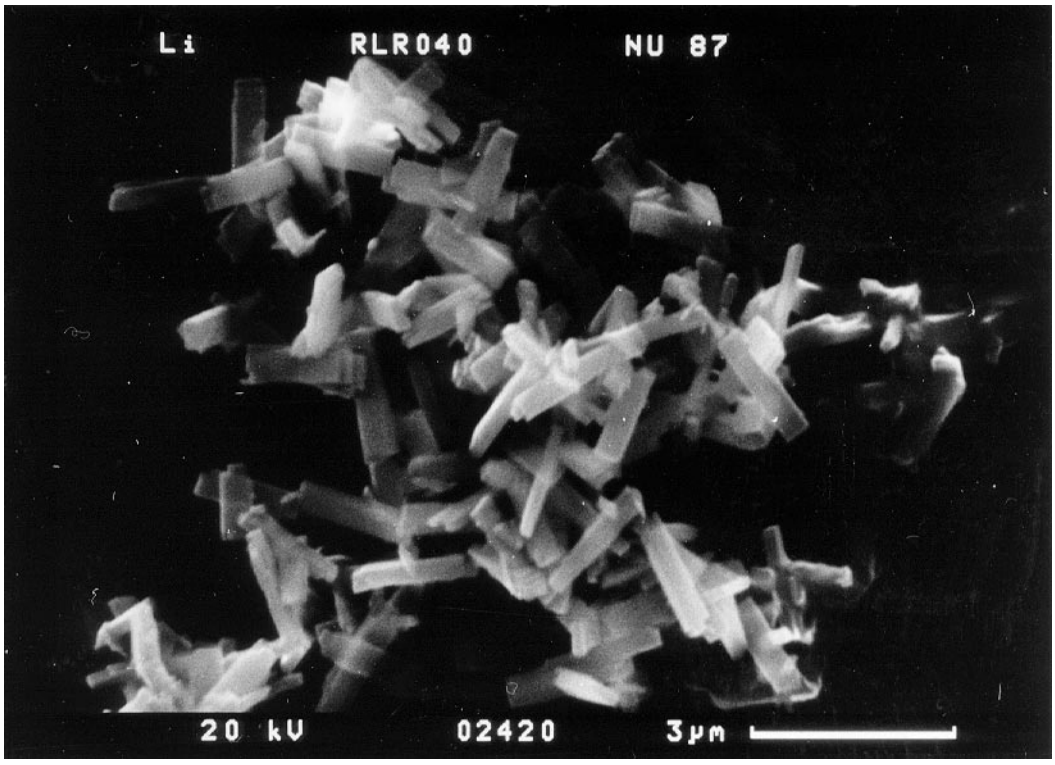

Figure 2. Scanning electron micrograph of zeolite NU-87 after calcination.

it can be deduced that NU-87 and SSZ-37 probably possess the same framework topology. From the scanning electron micrograph depicted in figure 2 it can be seen that the crystallites of zeolite NU-87 have a morphology of rectangular rods with sizes of ca. 1.5 μm $\times$ 2.0 μm.

In agreement with earlier data reported by Casci et al. [2], thermal analysis of as-synthesized NU-87 revealed that the weight loss upon heating in an air flow occurs in three steps. While the first (endothermic) step (completed at ca. 250°C) can be assigned to the desorption of water, the two additional steps (from 250 to 500°C and from 500 to 700°C) are exothermic and can be related to the combustion of the organic template. This observation suggests that the template is present either

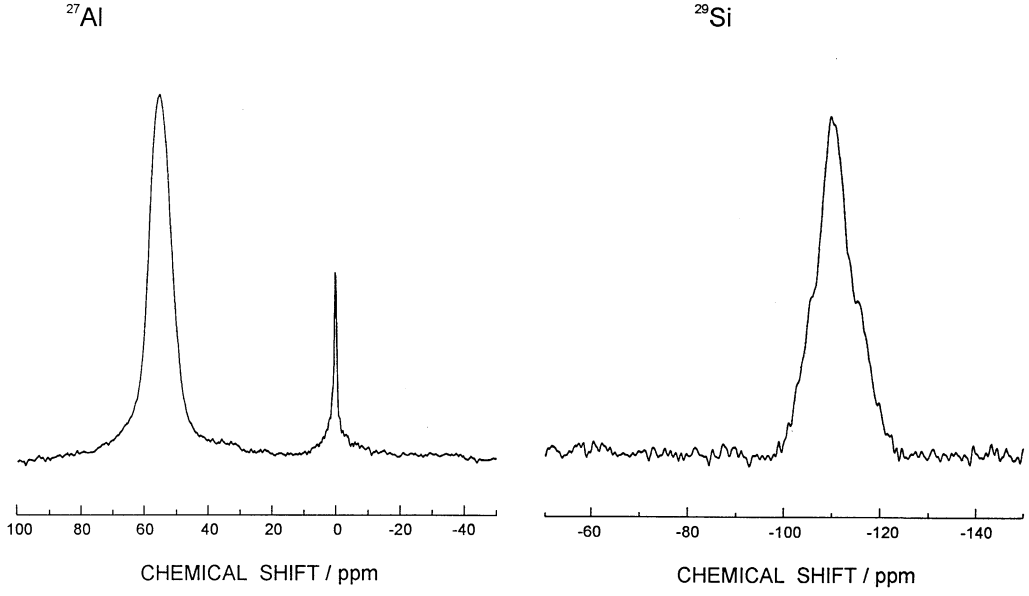

Figure 3. ^{27}Al and ^{29}Si MAS NMR spectra of zeolite NU-87 after calcination.

in two different configurations or at two different locations. Combustion of the free template (decamethonium bromide) occurs at temperatures around 300°C, hence part of the zeolite-occluded template seems to be considerably stabilized by host/guest interactions. In addition, it can be concluded from ^{13}C CP/MAS NMR spectroscopy that the template remains unchanged upon its occlusion in the zeolite pores. Thermal together with chemical analysis of the as-synthesized product yields the following composition (based on 68 T-atoms per unit cell [3]): $[(SiO_2)_{64.8}(AlO_2)_{3.2}(Na_2O)_{0.3}(Dec)_{1.8}(H_2O)_3]$. The unit cell formula indicates an enrichment of aluminum in the zeolite with respect to the synthesis gel and an excess of cations. It has to be considered that part of the tetraalkylammonium moieties of the decamethonium ions do not serve as charge-compensating cations but as void-filling species which might also be reflected by the thermal analysis data given above.

The ^{27}Al and ^{29}Si MAS NMR spectra of zeolite NU-87 after calcination are presented in figure 3. A relatively small signal around 0 ppm in the ^{27}Al spectrum (which is absent in the spectrum of the as-synthesized form) reveals that a minor part of the aluminum was removed from framework sites during calcination. A broad signal centered around 110 ppm in the ^{29}Si spectrum is indicative of crystallographically different T-sites for Si in the structure of NU-87.

The results of the temperature-programmed desorption of pyridine obtained for the zeolites HNU-87 and HMCM-22 with nearly the same n_{Si}/n_{Al}-ratio are shown in figure 4. As expected from the same n_{Si}/n_{Al}-ratio, the total number of desorbed pyridine molecules and, hence, the density of acid sites is comparable for both zeolites. However, the distribution of their strengths is different. It can be seen from figure 4 that zeolite HNU-87 possesses weakly acidic sites (maximum around 280°C) as well as a large number of very strongly acidic sites (maximum around 650°C). The pyridine desorption profile of zeolite HMCM-22 also shows a maximum around 280°C, but compared to zeolite HNU-87 the high-temperature maximum is somewhat broader and located at a lower temperature (maximum around 610°C). In other words, the strongly acidic sites in zeolite HMCM-22 possess a lower strength and a broader strength distribution as compared to those in zeolite HNU-87. The fact that the relative partial pressure of pyridine desorbed from HMCM-22 in the temperature range between the low- and the high-temperature maximum stays on a relatively high level suggests the existence of another type of acid sites of intermediate acid strength. A similar type of acid sites of comparable strength, but of lower density than in zeolite HMCM-22 seems to be present in zeolite HNU-87, too. This is in accordance with an earlier study of the acidity of zeolite HMCM-22 using temperature-programmed desorption of ammonia [9]. In this investigation the deconvoluted peaks of the ammonia desorption profile were tentatively assigned to three kinds of acid sites, i.e., weakly acidic Lewis sites, strongly acidic Brønsted sites and very strongly acidic Lewis sites. From the TPDP-measurements alone, however, no conclusion on the nature of the acid sites (Brønsted vs. Lewis) can be drawn.

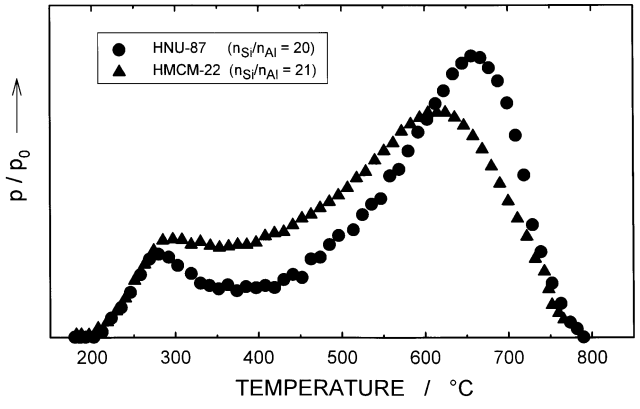

Figure 4. Temperature-programmed desorption of pyridine (TPDP) from zeolite HNU-87 ($n_{Si}/n_{Al} = 20$) and from zeolite HMCM-22 ($n_{Si}/n_{Al} = 21$), (heating rate 5 K/min, p/p_0 is the partial pressure of desorbed pyridine relative to the loading pressure $p_0 = p_{pyridine} = 1.3$ kPa).

Pyridine is also more strongly held by the strongly acidic sites of zeolite HNU-87 as compared to those of zeolite HBeta, which exhibits a desorption maximum at around 630°C, but none at lower temperatures (not shown). Since the strength of acid sites in zeolite HBeta lies between those of the zeolites HZSM-5 and HY [11], zeolite HNU-87 resembles HZSM-5 rather than HY with respect to the strength of its acid sites.

3.2. Conversion of methylnaphthalenes over zeolite HNU-87

2-methylnaphthalene was first chosen as a reactant, since mass transport limitations, if present, can be expected to be less pronounced than with 1-methylnaphthalene. Two main reactions can occur during the acid-catalyzed conversion of 2-methylnaphthalene, viz. isomerization to 1-methylnaphthalene and transalkylation/disproportionation to naphthalene and dimethylnaphthalenes.

Typical results obtained in the conversion of 2-methylnaphthalene on zeolite HNU-87 at 300°C are depicted in figure 5. The conversion declines slowly with time-on-stream, and a steady state is never reached. A similar loss in catalyst activity has been reported previously for the conversion of 1-methylnaphthalene over a number of zeolite catalysts including zeolites with 10-membered-ring pores, e.g., HZSM-5 and HEU-1, as well as zeolites with 12-membered-ring pores, e.g., HZSM-12 and HBeta [6]. On zeolite HNU-87, isomerization and transalkylation proceed at comparable rates. The yields of the transalkylation products are of the same order of

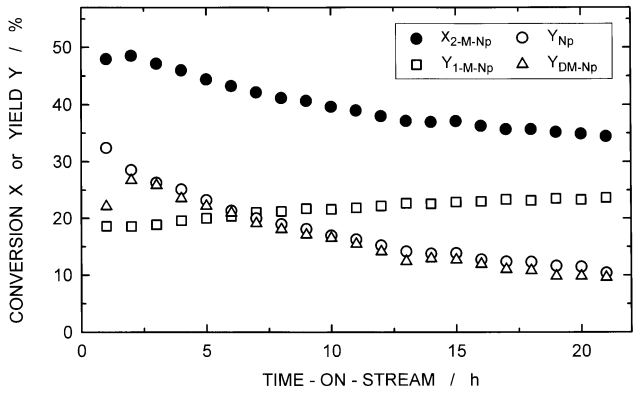

Figure 5. Conversion (X) and yields (Y) in dependence of time-on-stream for the reaction of 2-methylnaphthalene over zeolite HNU-87 at 300°C ($W/F_{2\text{-M-Np}} = 1970$ g h/mol, $p_{2\text{-M-Np}} = 0.2$ kPa).

magnitude as those obtained over zeolites HY or HZSM-20 [6], which possess a spacious pore system (spaciousness index SI ≈ 20 [12]). Over 12-membered-ring zeolites with a less spacious pore system, e.g., H-mordenite (SI = 7) or HZSM-12 (SI = 3), and 10-membered-ring zeolites, e.g., HEU-1 (SI = 3) and HZSM-5 (SI = 1), essentially no transalkylation products were observed in the conversion of 1-methylnaphthalene, whereas the catalysts were very active for isomerization [6,13]. These results were accounted for by transition state shape selectivity. It can thus be concluded, that the bulky transition states neccessary for the bimolecular transalkylation reaction can be accommodated in the 12-membered-ring cavities of zeolite HNU-87, but not in its 10-membered-ring pores. Nevertheless, the dimethylnaphthalenes formed can diffuse through these pores and finally leave the zeolite crystallites. It can be seen from figure 5 that, except at the beginning of the experiment, the yield ratio of naphthalene and dimethylnaphthalenes is close to unity, as one would expect from the stoichiometry of the transalkylation reaction. On zeolite HY, this ratio has been found to be $Y_{\text{Np}}/Y_{\text{DM-Np}} = 2$ at 300°C even after 6 h time-on-stream [13]. To account for such a deficit in dimethylnaphthalenes, consecutive reactions to higher molecular products have been invoked [13]. For reasons unknown so far, such reactions are absent in zeolite HNU-87.

It is furthermore seen from figure 5 that isomerization and transalkylation are differently affected by catalyst deactivation. While the rate of transalkylation decreases with time-on-stream, the rate of isomerization even slightly increases. This difference in the rates of isomerization and transalkylation and the difference in the yields of naphthalene and dimethylnaphthalenes at the beginning of the experiment will be addressed in the following chapter.

3.2.1. Influence of the modified residence time and the reaction temperature

The influence of the residence time on the conversion and yields after 5 h time-on-stream at a reaction temperature of 300°C is shown in the left-hand part of table 1. With increasing residence time, both the conversion and the yields of the transalkylation products increase almost linearly. At the same time, the yield of 1-methylnaphthalene decreases. If compared at the same conversion, e.g., at $X_{2\text{-M-Np}} = 40\%$ ($Y_{1\text{-M-Np}} = 21.4\%$, $Y_{\text{Np}} = 17.0\%$, $Y_{\text{DM-Np}} = 16.5\%$), reached at different times-on-stream for different residence times, the yields of the products are identical. Furthermore, the rate of deactivation, i.e., the decrease in conversion within a given time-on-stream, is the same for all modified residence times applied.

Similar effects occur if the reaction temperature is varied (table 1, right-hand part): Upon increasing the reaction temperature, both the conversion and the yields of the transalkylation products increase again, while the yield of the isomerization product 1-methylnaphthalene decreases. Furthermore, the difference between the yields of naphthalene and dimethylnaphthalenes increases significantly upon increasing the reaction temperature. This difference is highest at the beginning of an experiment and declines with time-on-stream. At 400°C, for example, the yield ratio of naphthalene and dimethylnaphthalenes decreases within ca. 10 h time-on-stream to reach a value close to unity, which remains virtually unchanged from then on (figure 6). It can be excluded that the excess of naphthalene over dimethylnaphthalenes within the first hours of the experiment is due to dealkylation of methylated naphthalene, since no methane, ethane, ethene or other aliphatic hydrocarbons were found in the product mixture, even though it was ascertained that they could have been detected, if they had formed. Although an induction period could in principle occur, it is unlikely that it is responsible for the naphthalene excess. An induction period has been observed for methylnaphthalene transalkylation over large pore zeolite catalysts at temperatures below 250°C only [13]. We rather believe that consecutive reactions of the transalkylation products have to be considered: This is particularly the case for the dimethylnaphthalenes which have the highest molecular weight of all hydrocarbons involved. It is reasonable to envisage a competitive

Table 1
Influence of reaction temperature and modified residence time (achieved by varying the mass of catalyst) on conversion (X, in %) and yields (Y, in %) in the reaction of 2-methylnaphthalene over zeolite HNU-87 after 5 h time-on-stream ($p_{2\text{-M-Np}} = 0.2$ kPa)

	$T_R = 300$°C, $W/F_{2\text{-M-Np}}$ (g h/mol)			$W/F_{2\text{-M-Np}} = 1970$ g h/mol, T (°C)			
	1009	1970	4028	300	350	400	450
$X_{2\text{-M-Np}}$	38.7	44.4	52.8	44.4	51.4	58.5	61.5
$Y_{1\text{-M-Np}}$	21.6	20.0	16.6	20.0	18.5	16.3	15.3
Y_{Np}	15.3	23.2	31.7	23.2	31.4	42.3	48.4
$Y_{\text{DM-Np}}$	14.3	22.4	32.8	22.4	29.7	36.2	37.8